

A NEW APPROACH TO LOAD TRANSFER IN BOLTED JOINTS

V. Weissberg . K. Wander . R. Itzhakov

Engineering Department

Israel Aircraft Industries Ltd.

Ben Gurion Airport, Lod, Israel.

Abstract

A series of tests on bolted single shear joints was performed, the test parameters being the bolt diameter and the tightening torque on the bolts. The test results were recorded on load-deflection diagram. Two distinct zones can be found on the typical load-deflection diagram; a friction zone and an elastic zone. It was shown that the amount of shear load transferred by the friction mechanism is proportional to the tightening torque. A typical friction coefficient was computed from the test data. The elastic part of the joint stiffness obtained from the deflection curve was represented on a non-dimensional diagram from which the elastic bolt stiffness can be obtained for any geometry or material. When the interplate friction forces were introduced into the plate displacement equilibrium equation, the result was to reduce, or truncate, the bolt shears, (and consequently the plate bearing and hoop-tension stresses).

The test results may be used to improve the accuracy of fatigue and damage tolerance analyses of bolted lap joints.

A three dimensional finite element analysis using contact non-linear elements was performed to obtain the joint stiffness, which showed good agreement with the elastic part of the test results. By means of this finite element model one can also evaluate the loads at the bolt-plate interface, which are otherwise unmeasurable. This will be the subject for further investigations.

I. Introduction

The accurate analysis of fastened joints is an important aspect in the efficient design of aircraft structures where minimum weight is a prime consideration. As a first step in such an analysis, it is necessary to know the distribution of the loads among the different fasteners in a multi-fastener joint. An important factor in the analysis of fastener load distribution in a multi-row joint is the shearing stiffness of each fastener in the assembly. This shearing stiffness can be obtained experimentally during tangential loading of a lap-joint from the resulting load-deflection diagram. (See MIL-STD-1312). The interpretation of this diagram can give valuable information about the load transfer

mechanism between the fastener and plate. In the 1950's when aircraft fatigue problems were being investigated, the major aircraft companies were attempting to analyze the shear splice flexibilities in order to obtain the individual fastener shear loads (1-3). Fig.1 gives a comparison of fastener flexibilities obtained by different companies.

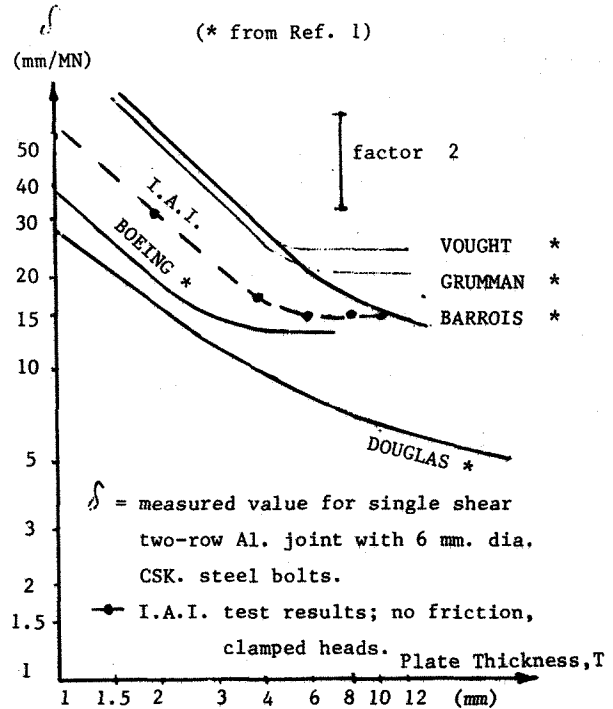


Figure 1. Comparison of Fastener Flexibility δ_f obtained by Different Companies

It is well known that the flexibility is influenced by the fastener geometry and material. From tests done at IAI it appears that the bolt tightening torque has a significant effect on the apparent flexibility. Since this effect is not usually accounted for, this may explain the large flexibility scatter observed in Fig. 1. It is found that a high torque reduces the apparent bolt flexibility because of friction. This friction effect is

also mentioned in (4). The approach in this paper is to represent the apparent joint stiffness as a function of the applied load. For this purpose a series of tests on bolted single lap joints was performed, from which an accurate load-deflection diagram was obtained. Parallel to this testing program, a three dimensional finite element analysis was performed.

II. Test Procedure

A series of tests was performed on 2-bolt lap-shear joints, to measure the bolt shear flexibilities. Eight joint configurations were tested. Each configuration is described in Figure 2 and Table 1. Seven configurations were with countersunk bolts (1/4" to 9/16" diameter, NAS 1972 series bolts and MS21045 nuts). The plate thickness was 1/2" for all the specimens. It was convenient to describe the joint characteristics by a non-dimensional parameter, Z, defined in equation [1] and derived in Appendix A.

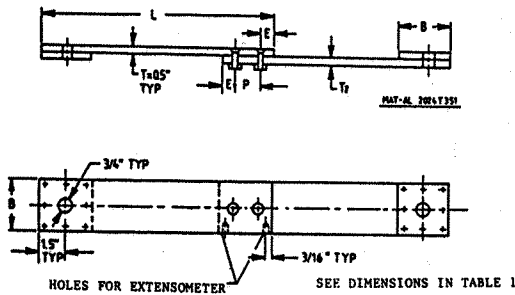


Figure 2. Test Specimen Geometry

Bolt and Nut	Diam. (in.)	L (in.)	B (in.)	E (in.)	P (in.)	T ₂ (in.)	Clear-ance (in.)	100% Torq. (lb. in.)
CSK Hd. Bolt NAS 1972 Nut MS 21045	1/4	9.0	2.0	1/2	1.	1/2	0.0015	125
	3/16	11.25	2.5	5/8	1.1/4	1/2	0.0015	250
	3/8	13.5	3.0	3/4	1 1/2	1/2	0.0015	430
	1/2	18.0	4.0	1.0	2.0	1/2	0.002	1210
	5/8	18.0	4.0	1.0	2.0	1.0	0.0015	1210
Hex Hd Bolt	1/2	18.0	4.0	1.0	2.0	1/2	interference from 0.0005 to 0.0015	1210
	5/8	20.25	4.5	1.1/4	2.1/4	1/2	0.002	1760

Table 1. Test Specimen Dimensions

Each test configuration corresponds to a different value of Z, which ranged from 0.2 (rigid bolts) to 2.8 (rigid plates).

$$Z = \left(\frac{T}{D}\right)^3 \cdot \frac{E_P}{E_B} \quad [1]$$

and

- Z - Non-Dimensional joint parameter ratio of bending stiffness of the bolt to plate bearing stiffness
- T - Thickness of the plate
- D - Diameter of the bolt
- E_P - Modulus of elasticity of the plate
- E_B - Modulus of elasticity of the bolt.

The tests were performed on an INSTRON machine, according to the MIL-STD-1312 method -4A. Displacements were measured by extensometer as shown in Fig 3. The test results were recorded on load-deflection plots. In order to obtain the effect of the tightening torque, the test was carried out as shown in the flow chart, Fig. 4. Three to five runs were performed on each specimen with different bolt tightening torques. The specimens were loaded up to 20%, 40%, and 60% of the expected ultimate load. Finally, the specimens were loaded up to failure.

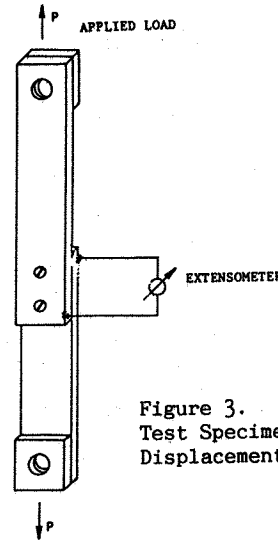


Figure 3. Test Specimen Displacement Measurements

Closing Torque Moment on Bolt (% of Max Torque) Applied Load Cycle (% of Expected Ultimate Load.)

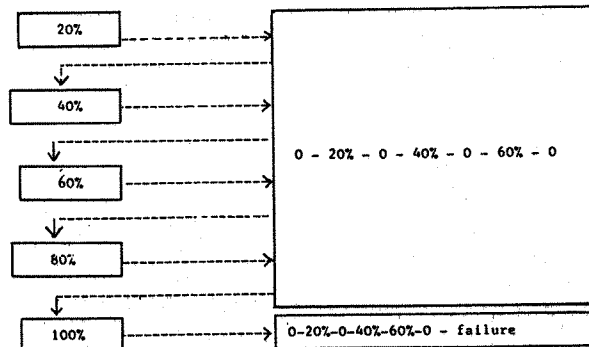


Figure 4. Flow Chart of Test Procedure

III. Test Results

The test results were recorded on load-deflection plots of extensometer deflections versus the applied load. In a typical load-deflection diagram, there are three distinct zones (see Fig. 5).

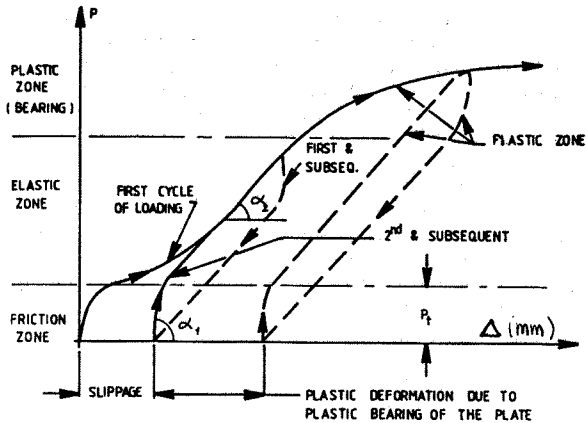


Figure 5. Typical Load-Displacement Curves

At the commencement of loading, the displacement slope, α_1 is very steep. In this zone, the displacement between the plates is restrained by the friction between the plates. When the applied load reaches value P_t (the transition value), the slope changes to α_2 . This slope is the bolt elastic stiffness when the sliding friction is exceeded. α_1 is the apparent friction stiffness of the joint. The value of P_t is significantly affected by the tightening torque.

Up to P_t , the load is transmitted by friction between the plates. P_t is therefore the static friction force. Above this value, the load is transmitted entirely by elastic contact between the plate and the bolt. From Fig. 5 one sees that the elastic joint stiffness is unaffected by the tightening torque. The slippage occurring during the first cycle is caused by the tendency of the bolts to align in the load direction and to close initial gaps. After the first cycle, the slippage effect is very small and can be ignored. The third zone is a zone of plastic bearing deformations, where the slope is further reduced.

If the load were reversed, the slippage would be expected to be twice the value of the slippage of the initial loading from zero. In this paper, there is no load reversal and the joint behaviour is considered only after the first cycle.

As stated above, the force P_t derived from the tests, represents the static interplate friction.

Now $P_t = \mu \cdot N$ [2]
 where N is the normal force due to the tightening torque

μ = the coefficient of static friction between the plates and can be derived from Data Sheets (5).

Then $\mu = P_t / N$ [3]
 where P_t is measured during the test.

The test result gave the following:

After the first cycle, $\mu \approx 0.3$.

This value of μ can then be used to calculate the value of P_t for any similar bolted joint.

α_2 is the elastic bearing joint stiffness, and $\frac{1}{\alpha_2}$ equals the compliance δ .

i.e. $\delta = \frac{1}{\alpha_2}$ [4]

The test results are represented by the non-dimensional diagram in Fig. 6.

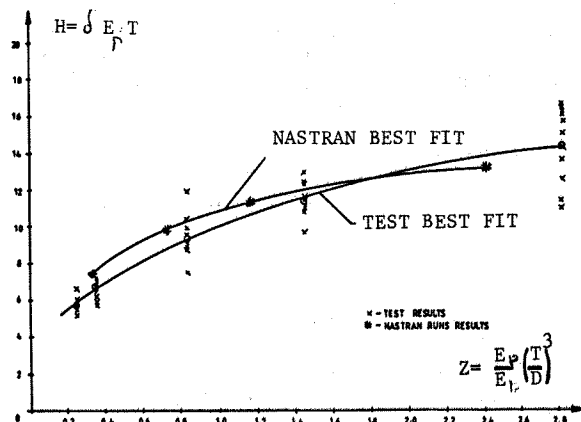


Figure 6. Non-Dimensional Diagram of Joint Compliance H vs. Configuration Parameter Z

The nondimensional joint compliance is given by

$$H = E_p \cdot \delta \cdot T \quad [5]$$

and this is plotted against the non-dimensional joint parameter, Z , equation [1].

When friction is taken into account, the apparent joint compliance is equal to the displacement divided by the load, and this value changes continuously with the load. Different literature sources (see Fig. 1) have used different methods to derive the compliance, i.e. with and without the friction part of the load-displacement curve.

The Vought and Grumman curves in the figure agree with our test results in the frictionless elastic zone (Fig. 1). The Douglas and Boeing curves agree roughly with the IAI apparent joint compliance at the bearing yield load.

IV. Calculation of Net Bolt Shear Load Distribution

Consider a 3-bolt single shear lap joint with friction (Fig. 7).

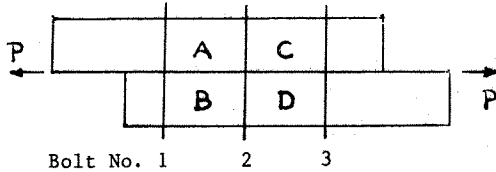


Figure 7. Bolt Lap-Shear Configuration

Let R_i ($i = 1 \rightarrow 3$), be the net shear forces for bolts 1, 2, 3 respectively (without friction).

These are the unknowns which must be determined.

R_{0i} ($i=1 \rightarrow 3$) are the interplate static friction forces, due to bolt tightening which are assumed to be concentrated at bolts 1, 2, 3 respectively. These forces are identical to P_t which is determined experimentally. When the external load P exceeds the total static friction, $\sum R_{0i}$, interplate sliding occurs. The friction forces are assumed to remain constant, and then $P = \sum R_{0i} + \sum R_i$

Three equations are written to solve for Force Equilibrium :-

$$R_1 + R_2 + R_3 = P - R_{01} - R_{02} - R_{03} \quad [6]$$

Displacement Compatibility for segments A and B :

$$(F_B + \delta_1 + F_A)R_1 - \delta_2 R_2 = R_{01}F_B + PF_A + R_{01}F_A \quad [7]$$

and for segments C and D :-

$$\delta_2 R_2 + (-F_D - F_C - \delta_3)R_3 = -PF_D + R_{03}F_D + R_{03}F_C \quad [8]$$

where δ_1 , δ_2 , and δ_3 are the bolt shear flexibilities, and F_A , F_B , F_C , and F_D are the segment flexibilities for segments A, B, C and D respectively (Fig. 7).

The friction effect is shown schematically in Fig. 8. When friction is present the bolt shears, R_i are reduced by the interplate friction, R_{0i} .

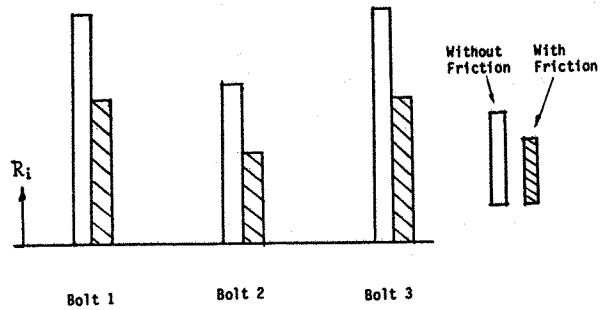


Figure 8. The Effect of Friction on the Bolt Shear Force R

Therefore under a fluctuating external load, P , the bolt shears, R_1 , R_2 , R_3 , will exhibit a truncated and slightly lagged version of P . This effect is shown schematically in Fig. 9.

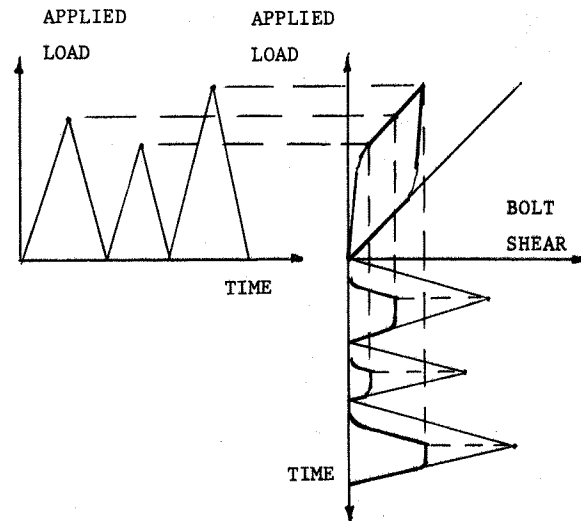


Figure 9. Truncated Bolt Shear Spectrum due to Bolt Torque Clamping Friction

This truncation due to friction means that the bolt shears and consequently the hoop-tension stresses around the bolt holes, are reduced, which improves the fatigue life of the joint.

V. Finite Element Model for Single Bolt

In parallel with the testing program, a three dimensional finite element analysis was performed. The finite element model (Fig.10) used HEXA solid elements. The plates and the bolt are represented by three free bodies interconnected by a contact element, GAP.

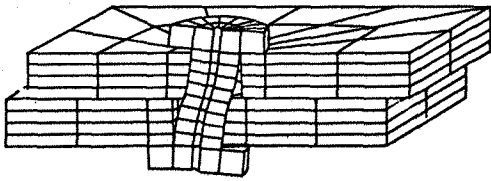


Figure 10. Finite Element Model of Single Bolt Joint

The model was run with the NASTRAN non-linear option (6). The non-linear solution was needed for the gap elements (see Appendix B), to solve for the bolt-to-plate contact.

The bolt and plates were assumed linear elastic, so that the finite element analysis gave the elastic zone behaviour. The results which are represented in Fig. 6 compare the analysis to test results. Good agreement is obtained for the joint stiffness comparison. This gives a high level of confidence in the accuracy of the analysis, which can then also be used to evaluate the otherwise unmeasurable loads at the bolt-plate interface, as shown in Fig. 11.

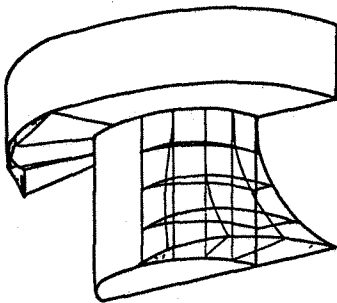


Figure 11. Pressure Distribution on the Bolt as obtained from F.E. Analysis

VI. Conclusions

A series of tests on bolted single lap shear joints was performed, the test parameters being the bolt diameter and the tightening torque on the bolts. Two distinct zones can be found on the typical load-deflection diagram; a friction zone and an elastic zone. It was shown that the amount of shear load transferred by the friction mechanism is proportional to the tightening torque. A typical friction coefficient was computed from the test data. The elastic part of the joint stiffness obtained from the load-deflection curve was represented on a non-dimensional diagram from which the elastic bolt stiffness can be obtained for any geometry

or material. When the interplate friction forces were introduced into the plate displacement equilibrium equation, the result was to reduce, or truncate, the bolt shears, (and consequently the plate bearing and hoop-tension stresses). The test results may be used to improve the accuracy of fatigue and damage tolerance analyses of bolted lap joints. A three dimensional finite element analysis using contact non-linear elements was performed to obtain the joint stiffness, which showed good agreement with the elastic part of the test results. By means of this finite element model one can also evaluate the loads at the bolt-plate interface, which are otherwise unmeasurable. This will be the subject for further investigations.

Acknowledgements

The authors wish to acknowledge the help of Mrs. Liza Lief in typing the manuscript, and Y. Geri and N. Cohen for performing the tests. Special thanks are due to Dr. A. Unger for his useful suggestions.

References

1. Huth, H., "Influence of Fastener Flexibility on the Prediction of Load Transfer and Fatigue Life for Multiple-Row Joints," "Fatigue in Mechanically Fastened Composite and Metallic Joints," ASTM STP 927, John M. Potter, Ed., 1986, pp. 221-250.
2. H.G. Harris, I.U. Ojalvo, R.E. Hoodson, "Stress and Deflection Analysis of Mechanically Fastened Joints," AFFDL - TR - 70 - 49, May 1970.
3. W. Barrois, "The Use of General Fatigue Data in the Interpretation of Full-Scale Fatigue Tests." AGARD - AG - 228 set 1977.
4. L. Jarfall, "Shear Loaded Fastener Installation". ICAF 1983, France, Toulouse.
5. ESDU Data Sheet 72022. "Tension in Steel Bolts Resulting from Tightening Torque".
6. MSC/NASTRAN - User's and Application Manuals - The MacNeal-Schwendler Corporation, 1985.

APPENDIX A

The Non-Dimensional Representation of Shearing Stiffness

In order to simplify and organize the test results, it is convenient to make a non-dimensional representation of the shearing stiffness as a function of the joint parameters. This representation is based on the assumption that the interaction between the bolt and plate is determined by the ratio of the bending stiffness of the bolt to the bearing stiffness of the plate. The non-dimensional value Z defined below contains both geometric and material properties of the plate and bolt that characterize the joint :

$$Z = \frac{\text{Bending Stiffness of the Fastener}}{\text{Bearing Stiffness of the Plate}}$$

Consider two limiting cases (see Fig. 12).

- (a) Low plate stiffness or infinite bolt stiffness; $Z \rightarrow \infty$
- (b) Low bolt stiffness or infinite plate stiffness; $Z \rightarrow 0$

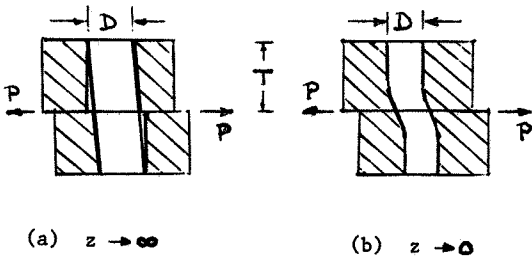


Figure 12. Limiting Cases of Bolt-Plate Interactions

Let $K = 1/\delta =$ Joint shearing stiffness.
If $K (Z \rightarrow \infty) = D \cdot E_p \cdot C_1 =$ Bearing Stiffness of Plate

where C_1 is a constant ($= 1.25$ for infinite plate) (3)

and $K (Z \rightarrow 0) = \frac{3E_b I_b}{T^3} =$ Bending stiffness of Bolt

where $I_b =$ Moment of Inertia of Bolt $= \frac{\pi D^4}{64}$

and $T =$ Thickness of Plate, as previously defined, then :-

$$K(Z \rightarrow 0) = \frac{3E_b \pi D^4}{64 T^3}$$

From equations,

$$Z = \frac{K(\text{Bearing}, z \rightarrow \infty)}{K(\text{Bending}, z \rightarrow 0)} = \frac{64 C_1 E_p T^3}{3 E_b \pi D^3} = \frac{E_p T^3}{E_b D^3} \cdot C_o$$

where $C_o = 64 C_1 / 3$
and $H_o =$ Non-Dimensional Joint Flexibility
 $= E_p T / K = E_p T \cdot \delta$

The joint compliance will therefore be represented in the non-dimensional form in the table and figures of this paper.

APPENDIX B

Contact Element GAP

The GAP element is intended to model surfaces which may come into contact with each other. It is used to connect two points of different bodies in contact. When these bodies disconnect, the GAP element transfers no load, and when the bodies approach, the GAP element connects the two points. The GAP element (Fig. 13) has two springs, A and B, and an initial gap U. In our case we assume $U = 0$, $K_A \rightarrow \infty$ and $K_B \rightarrow 0$, where K_A and K_B are the spring constants of A and B respectively. When the two points, G_1 and G_2 , tend to separate, U tends to increase and only the spring B transfers load. Since $K_B = 0$, the resistance will be close to zero. When the two points G_1 and G_2 tend to approach, U tends to decrease and the two springs, A and B, will transfer load. Since $K_A \rightarrow \infty$ the GAP element represents a rigid contact between the two points. This contact will depend on the geometry and stiffness of the two bodies in contact.

In our particular case we assume that U represents the contact of the bolt shank with the hole in the radial direction, and the contact of the bolt head with the plate in the vertical direction.

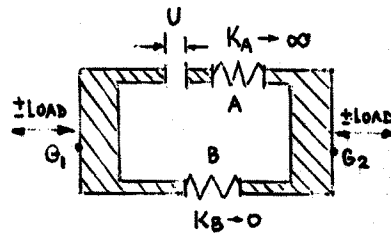


Figure 13. Schematic Diagram of a GAP Element